

Evolution of spherical over-densities in tachyon scalar field model

M. R. Setare*

Department of Science, Campus of Bijar, University of Kurdistan, Bijar, Iran.

F. Felegary[†] and F. Darabi[‡]

Department of Physics, Azarbaijan Shahid Madani University, Tabriz, 53714-161 Iran

(Dated: March 4, 2022)

We study the tachyon scalar field model in flat FRW cosmology with the particular potential ϕ^{-2} and the scale factor behavior $a(t) = t^n$. We consider the spherical collapse model and investigate the effects of the tachyon scalar field on the structure formation in flat FRW universe. We calculate $\delta_c(z_c)$, $\lambda(z_c)$, $\xi(z_c)$, $\Delta_V(z_c)$, $\log[\nu f(\nu)]$ and $\log[n(k)]$ for the tachyon scalar field model and compare the results with the results of EdS model and Λ CDM model. It is shown that in the tachyon scalar field model the structure formation may occur earlier, in comparison to the other models.

PACS numbers: 98.80.-k; 95.36.+x; 04.50.Kd.

I. INTRODUCTION

The last cosmological and astrophysical data of Large Scale structure, the observations of type Ia and Cosmic Microwave Background radiation have demonstrated that currently there is an acceleration expansion phase in the universe [5, 20]. The cosmic expansion can be well described by a negative pressure so-called dark energy (DE). The simplest candidate for DE is the cosmological constant. However, the cosmological constant suffers from the fine-tuning and the cosmic coincidence problems [7],[26]. Therefore, to avoid these problems, different models for dark energy have been proposed such as quintessence, K-essence, tachyon [22], ghost [29], phantom, quintom [6], and the quantum gravity models, as well as holographic [30] and new agegraphic models [7], [16]. The tachyon model as a scalar field model arises in particle physics and string theory. Thus, it can be considered as one of the potential candidates to describe the nature of the DE.

On the other hand, the problem of structure formation in the universe is a very important issue in theoretical cosmology. A simple model of structure formation is the spherical collapse model. The spherical collapse model was presented by Gunn and Gott [10]. This model studies the evolution of growth of overdense structures with respect to the dynamics of scale factor or cosmic redshift. The dynamics of overdense structures depends on the dynamics of the background Hubble flow and expansion of the universe. In the frame of general relativity, the spherical collapse model has been studied [9],[11],[21]. In this paper, we study the spherical collapse and the evolution of spherical overdensities in the framework of tachyon scalar field model and compare the results with the results of Einstein-de Sitter (EdS) and Λ -Cold Dark Matter (Λ CDM) models.

II. COSMOLOGY WITH TACHYON SCALAR FIELD

The Lagrangian of tachyon scalar field over a cosmological background is given by [28]

$$\mathcal{L} = -V(\phi)\sqrt{1 - \partial_a\phi \partial^a\phi}, \quad (1)$$

where ϕ and $V(\phi)$ are the tachyon scalar field and tachyon potential, respectively, and we consider the Friedmann-Robertson-Walker (FRW) metric having the cosmic time t dependent scale factor $a(t)$. For a

*Electronic address: rezakord@ipm.ir

[†]Electronic address: falegari@azaruniv.ac.ir

[‡]Electronic address: f.darabi@azaruniv.ac.ir; Corresponding -author

homogeneous field, the equation of motion is obtained as

$$\frac{\ddot{\phi}}{1 - \dot{\phi}^2} + 3H\dot{\phi} + \frac{\dot{V}(\phi)}{V(\phi)} = 0, \quad (2)$$

where the symbols \cdot and $'$ denote the derivatives with respect to t and ϕ , respectively, and $H = \dot{a}/a$ is called the Hubble parameter. In the flat FRW universe, the energy density ρ_Λ and the pressure p_Λ of the tachyon field read as

$$\rho_\Lambda = \frac{V(\phi)}{\sqrt{1 - \dot{\phi}^2}}, \quad (3)$$

$$p_\Lambda = -V(\phi)\sqrt{1 - \dot{\phi}^2}. \quad (4)$$

For the pressureless matter and tachyon scalar field matter, the Friedmann equation is given by

$$H^2 = \frac{1}{3M_{pl}^2}(\rho_m + \rho_\Lambda), \quad (5)$$

where ρ_Λ is the energy density of tachyon scalar field, and ρ_m is the density of pressureless matter. We suppose that there is no interaction between ρ_Λ and ρ_m , so the continuity equations are given separately by

$$\dot{\rho}_\Lambda + 3H\rho_\Lambda(1 + \omega_\Lambda) = 0, \quad (6)$$

$$\dot{\rho}_m + 3H\rho_m = 0. \quad (7)$$

Using Eqs. (3) and (4) and also $p_\Lambda = \omega_\Lambda\rho_\Lambda$, the equation of state parameter (EoS) for tachyon scalar field is obtained as

$$\omega_\Lambda = \dot{\phi}^2 - 1. \quad (8)$$

The requirement for a real ρ_Λ results in $0 < \dot{\phi}^2 < 1$ according to which ω_Λ should vary as $-1 < \omega_\Lambda < 0$. The fractional energy densities are defined by

$$\Omega_\Lambda = \frac{\rho_\Lambda}{3M_{pl}^2 H^2}, \quad (9)$$

$$\Omega_m = \frac{\rho_m}{3M_{pl}^2 H^2}. \quad (10)$$

Taking time derivative of Eq. (9) and using Eq. (6) yields

$$\dot{\Omega}_\Lambda = -\Omega_\Lambda H \left[3(1 + \omega_\Lambda) + 2\frac{\dot{H}}{H^2} \right]. \quad (11)$$

Also, taking time derivative of Eq. (5) and using Eqs. (6) and (7) yields

$$2\frac{\dot{H}}{H^2} = -3(1 + \omega_\Lambda\Omega_\Lambda). \quad (12)$$

Using Eq. (12) and inserting Eq. (11), we obtain

$$\dot{\Omega}_\Lambda = 3\omega_\Lambda\Omega_\Lambda(\Omega_\Lambda - 1). \quad (13)$$

Here, the prime is the derivative with respect to $x = \ln a$ where $a = (1+z)^{-1}$ and z is the cosmic redshift. Using $\frac{d}{dx} = -(1+z)\frac{d}{dz}$ and Eq. (8), one finds

$$\frac{d\Omega_\Lambda}{dz} = -3\Omega_\Lambda(\Omega_\Lambda - 1)(\dot{\phi}^2 - 1)(1+z)^{-1}. \quad (14)$$

The differential equation for the evolution of dimensionless Hubble parameter, $E(z) = \frac{H}{H_0}$, in tachyon scalar field model, is obtained by using Eqs. (6), (7), (8) and (12) as follows

$$\frac{dE}{dz} = \frac{3}{2} \frac{E}{(1+z)} \left[1 + \Omega_\Lambda(\dot{\phi}^2 - 1) \right]. \quad (15)$$

Now, we consider the following particular potential which results in the scalar field with linear time dependence and the scale factor with suitable power law behaviour, as follows [28]

$$V(\phi) = \frac{2n}{M_{pl}^2} \left(1 - \frac{2}{3n} \right)^{\frac{1}{2}} \frac{1}{\phi^2}, \quad (16)$$

$$\phi = \sqrt{\frac{2}{3n}} t, \quad (17)$$

$$a(t) = t^n. \quad (18)$$

Taking time derivative of Eq. (17), inserting in Eq. (8) and using Eq. (18), we can obtain the equation of state parameter for tachyon scalar field model

$$\omega_\Lambda = \frac{2}{3n} - 1. \quad (19)$$

In Eq. (19), we can see that if $n \geq \frac{2}{3}$, then we will have $-1 < \omega_\Lambda < 0$. Using Eq. (19) and inserting it in Eqs. (14), (15) we can get the evolution of EoS parameter (ω_Λ), the density parameter of dark energy (Ω_Λ), and the dimensionless Hubble parameter ($E(z)$) in tachyon scalar field model as a function of cosmic redshift. In Fig.1, assuming the present values $\Omega_{\Lambda_0} \approx 0.7$, $\Omega_{m_0} \approx 0.3$ and $H_0 \approx 67.8 \frac{km}{sMpc}$, we have shown the evolution of EoS parameter, the evolution of density parameter and the evolution of dimensionless Hubble parameter of tachyon scalar field model with respect to the redshift parameter z for the typical value $n = 1$.

III. LINEAR PERTURBATION THEORY

In this section, we study the linear growth of perturbation of non relativistic dust matter by computing the evolution of growth factor $g(a)$ in tachyon scalar field model, and then compare it with the evolution of growth factor in EdS and Λ CDM models. The differential equation for the evolution of the growth factor $g(a)$ is given by [13],[14],[18] (see Appendix I)

$$g''(a) + \left(\frac{3}{a} + \frac{E'(a)}{E(a)} \right) g'(a) - \frac{3}{2} \frac{\Omega_{m_0}}{a^5 E^2(a)} g(a) = 0. \quad (20)$$

In order to study the linear growth in tachyon scalar field model, using Eqs.(14), (15) and (19) for $n = 1$, we solve numerically Eq.(20). To obtain the linear growth of structures in the EdS model and the Λ CDM model, we use the procedure used in Ref [30]. In figure (2), we have plotted the evolution of growth factor $g(a)$ with respect to the scale factor. At first, namely for small scale factors, the growth factor in the tachyon scalar field model is larger than those of EdS and Λ CDM models. However, for rather larger scale factors, the growth factor in the tachyon scalar field model becomes smaller than the EdS model while it is still larger enough than that of Λ CDM model. This means that, at the beginning, the tachyon scalar field model predicts structure formation more efficient than EdS and Λ CDM models. For later times, however, the structure formation in the tachyon scalar field model is dropped behind that of EdS model, whereas it precedes the structure formation in the Λ CDM model.

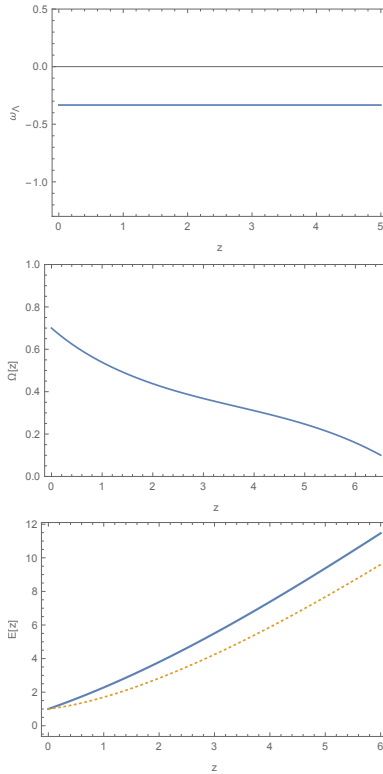


FIG. 1: The evolution of EoS parameter (top), dark energy density parameter (middle), and dimensionless Hubble parameter (down) of tachyon scalar field model with respect to the redshift parameter z . The thick line represents the tachyon scalar field model for $n = 1$ and the dotted line shows the Λ CDM model.

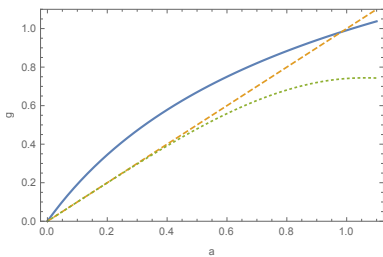


FIG. 2: Time evolution of the growth factor as a function of the scale factor. The thick line represents the tachyon scalar field model for $n = 1$. The dotted line indicates the Λ CDM model and the dashed line represent the EdS model.

IV. SPHERICAL COLLAPSE IN THE TACHYON SCALAR FIELD MODEL

The structure formation is described by a non-linear differential equation for the evolution of the matter perturbation δ in a matter dominated universe [4],[15]. In [1] this differential equation was generalized to the case of evolution of δ in a universe including a dark energy component. Now, we consider the non-linear differential equation which is given by [13] (see Appendix I)

$$\delta'' + \left(\frac{3}{a} + \frac{E'(a)}{E(a)} \right) \delta' - \frac{4}{3} \frac{\delta'^2}{1 + \delta} - \frac{3}{2} \frac{\Omega_{m0}}{a^5 E^2(a)} \delta(1 + \delta) = 0, \quad (21)$$

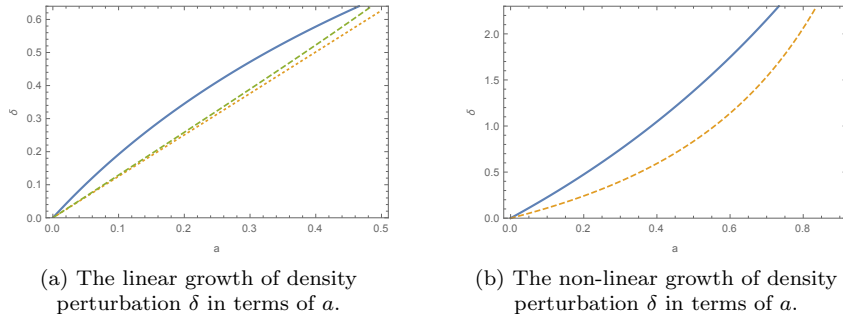


FIG. 3: The thick line represents the tachyon scalar field model for $n = 1$. The dotted line indicates the Λ CDM model and the dashed line indicates the EdS model.

where $'$ denotes the derivative with respect to a . In the linear regime, we have

$$\delta'' + \left(\frac{3}{a} + \frac{E'(a)}{E(a)} \right) \delta' - \frac{3}{2} \frac{\Omega_{m_0}}{a^5 E^2(a)} \delta = 0. \quad (22)$$

In EdS model, we consider the initial conditions $\delta_i = 20.9 \times 10^{-4}$, $\delta'_i = 0$ and $a_i = 10^{-4}$ [13]. In order to study the linear growth of density perturbation and the non-linear growth of density perturbation in tachyon scalar field model, using Eqs.(14), (15) and (19) for $n = 1$, we solve numerically Eqs.(21) and (22) (see Appendix II). To obtain the linear growth of density perturbation δ in the EdS model and the Λ CDM model, we use the procedure used in Ref [30]. The figure (3-a) shows that the linear growth factor in the tachyon scalar field model is larger than those of EdS and the Λ CDM models, and the figure (3-b) shows that the non-linear growth factor in the tachyon scalar field model is larger than the EdS model.

V. DETERMINATION OF δ_c AND Δ_V

As time passes, the perturbation is growing and one can no longer use the linear regime. At this stage, the radius of perturbation region becomes maximal $R = R_{max}$ and the perturbation stops growing. This condition is called turn-around which points to the epoch when the growth of perturbation decouples from the Hubble flow of the homogenous background. After the turn-around the perturbation starts contracting. For a perfect spherical symmetry and perfect pressureless matter, the perturbation would collapse to a single point becoming infinitely dense. Since there is hardly any perfect spherical symmetric overdensity in the universe, the perturbation does not collapse to a single point and finally a virialized object of a certain finite size in equilibrium state is formed that is called halo.

We call (z_c, R_c) and (z_{ta}, R_{ta}) as the redshift and radius corresponding to virialization and the turn-around epochs, respectively. Now, we peruse two characterising quantities of the spherical collapse model for the tachyon scalar field model: the virial overdensity Δ_V and the linear overdensity parameter δ_c . We consider a spherical overdense region with matter density ρ in a surrounding universe described by its background dynamics and density ρ_b . The virial overdensity Δ_V is defined by [12]

$$\Delta_V = \frac{\rho}{\rho_b} \frac{R_c}{a_c}, \quad (23)$$

which is a function of scale factor and redshift. We can rewrite the virial overdensity Δ_V as follows [12]

$$\Delta_V = 1 + \delta(a_c) = \xi \left(\frac{x_c}{\lambda} \right)^3, \quad (24)$$

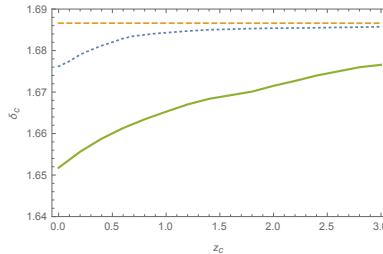


FIG. 4: The time evolution of the linear overdensity, $\delta_c(z)$, in terms of a function of the collapse redshift for the Λ CDM model, the EdS model and the tachyon scalar field model. The thick line represents the tachyon scalar field model for $n = 1$. The dotted line indicates the Λ CDM model and the dashed line indicates the EdS model.

where

$$x_c = \frac{a_c}{a_{ta}}, \quad (25)$$

$$\xi = \frac{\rho(R_{ta})}{\rho_b(a_{ta})} = 1 + \delta(a_{ta}). \quad (26)$$

Here, λ is the virial radius which is given by [25]

$$\lambda = \frac{1 - \frac{\eta_\nu}{2}}{2 + \eta_t - \frac{3}{2}\eta_\nu}, \quad (27)$$

where η_t and η_ν are the (Wang-Steinhardt) WS parameters

$$\eta_t = \frac{2 \Omega_\Lambda(a_{ta})}{\xi \Omega_m(a_{ta})}, \quad (28)$$

$$\eta_\nu = \frac{2 \Omega_\Lambda(a_c)}{\xi \Omega_m(a_c)} \left(\frac{a_{ta}}{a_c} \right). \quad (29)$$

Now, we discuss the results obtained for the linear overdensity parameter and the virial overdensity for the models introduced in this work. The figure (4) shows the time evolution of linear overdensity, $\delta_c(z)$ in terms of a function of the collapse redshift for the Λ CDM model, the EdS model and the tachyon scalar field model. In the EdS model, δ_c is independent of the redshift, hence it has a constant value i.e. $\delta_c = 1.686$. In the Λ CDM model, δ_c is smaller than 1.686 but the time evolution of the linear overdensity approaches the value of the EdS model at high redshifts.

In fact, at high redshifts we have a matter dominated universe (dust matter), but at lower redshifts we have a dark energy dominated universe, thus the structure formation must occur earlier. In the tachyon scalar field model, δ_c drives more slowly than the Λ CDM and the EdS models because in Fig.1, the Hubble parameter in the tachyon scalar field model is larger than that of Λ CDM model.

In the figure (5), we represent $\lambda(z_c)$ in terms of z_c for the Λ CDM model, the EdS model and the tachyon scalar field model. In the EdS model, $\lambda(z_c)$ is independent of the redshift, thus it has a constant value i.e. $\lambda = 0.5$. In the Λ CDM model, $\lambda(z_c)$ is smaller than 0.5 but it approaches the value of the EdS model at high redshifts. In the tachyon scalar field model, $\lambda(z_c)$ drives more slowly than the Λ CDM and the EdS models but its value approaches the value of the EdS model at high redshifts. Therefore, we can conclude that the size of structures in the Λ CDM model is larger than the tachyon scalar field model.

In the figure (6-a), we represent $\xi(z_c)$ in terms of z_c for the Λ CDM model, the EdS model and the tachyon scalar field model. In the EdS model, $\xi(z_c)$ is independent of redshift thus it has a constant value i.e. $\xi = 5.6$.

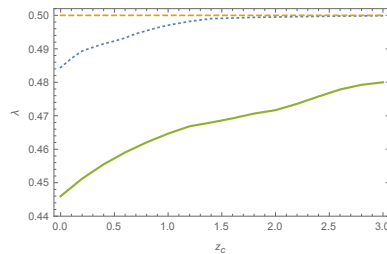
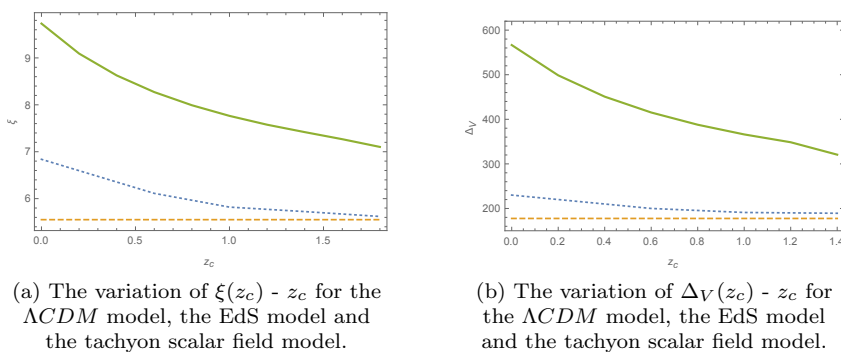


FIG. 5: The virial radius $\lambda(z_c)$ in terms of the collapse redshift z_c for the Λ CDM model, the EdS model and the tachyon scalar field model. The thick line represents the tachyon scalar field model for $n = 1$. The dotted line indicates the Λ CDM model and the dashed line indicates the EdS model.



(a) The variation of $\xi(z_c) - z_c$ for the Λ CDM model, the EdS model and the tachyon scalar field model.

(b) The variation of $\Delta_V(z_c) - z_c$ for the Λ CDM model, the EdS model and the tachyon scalar field model.

FIG. 6: The blue, green and red lines represent the tachyon scalar field model for $n = 0.9, 1, 1.1$, respectively. The dotted line indicates the Λ CDM model and the dashed line indicates the EdS model.

In the Λ CDM model, $\xi(z_c)$ is larger than 5.6 but its value approaches the value of the EdS model in terms of high redshifts. In the tachyon scalar field model, $\xi(z_c)$ drives faster than the Λ CDM model and the EdS model but its value approaches the value of the EdS model in terms of high redshifts. Therefore, we can conclude that in the tachyon scalar field model the overdense spherical regions in terms of z_c are denser than the Λ CDM model and the EdS model.

In the figure (6-b), we show the virial overdensity $\Delta_V(z_c)$ in terms of z_c for the Λ CDM model, the EdS model and the tachyon scalar field model. In the EdS model, $\Delta_V(z_c)$ is independent of redshift, thus it has a constant value, $\Delta_V = 178$. In the Λ CDM model, $\Delta_V(z_c)$ drives more faster than 178, but its value approaches the value of the EdS model in terms of high redshifts. In the tachyon scalar field model, $\Delta_V(z_c)$ drives faster than the Λ CDM model and its value approaches the value of the EdS model in terms of high redshifts. The evolution of virial overdensity parameter $\Delta_V(z_c)$ is the main quantity for the halo size. Therefore, we can conclude that in the tachyon scalar field model the halo size is larger than the EdS model and the Λ CDM model.

VI. NUMBER DENSITY AND MASS FUNCTION

The average comoving number density of halos of mass M is given by [3],[17]

$$n(M, z) = \left(\frac{\rho}{M^2}\right) \frac{d \log \nu}{d \log M} \nu f(\nu), \quad (30)$$

where $f(\nu)$ and ρ are the multiplicity function and the background density, respectively and ν is given by

$$\nu = \frac{\delta_c^2}{\sigma^2(M)}. \quad (31)$$

Here $\sigma(M)$ is the r.m.s of the mass fluctuation in sphere of mass M . We can use the formula given by [24]

$$\sigma(M, z) = \sigma_8(z) \left(\frac{M}{M_8} \right)^{-\frac{\gamma(M)}{3}}, \quad (32)$$

where σ_8 is the mass variance of the overdensity on the scale of R_8 , $M_8 = 6 \times 10^{14} \Omega_{m_0} h^{-1} M_\odot$ and $R_8 = 8h^{-1} Mpc$ are the mass and the radius inside a sphere. Also, $\sigma_8(z)$ is given by

$$\sigma_8(z) = g(z) \sigma_8(M, z = 0), \quad (33)$$

where $g(z)$ is the linear growth factor, $\sigma_{8,DE}(M, z = 0) = 0.8 \times \left(\frac{\delta_{c,DE}(z=0)}{\delta_{c,\Lambda CDM}(z=0)} \right)$ and

$$\gamma(M) = (0.3\Gamma + 0.2) \left[2.92 + \frac{1}{3} \log\left(\frac{M}{M_8}\right) \right], \quad (34)$$

where $\Gamma = \Omega_{m_0} h \exp(-\Omega_b - \frac{\Omega_b}{\Omega_{m_0}})$. Eqs. (32) and (34) have a validation range [24]. They express that the fitting formula predicts higher values of the variance for $M < M_8$ and the fitting formula predicts lower values of the variance for $M > M_8$. Following [23], we apply ST mass function

$$\nu f_{ST}(\nu) = 0.3222 \sqrt{\frac{0.707\nu}{2\pi}} \left[1 + (0.707\nu)^{-0.3} \right] \exp\left(-\frac{0.707\nu}{2}\right). \quad (35)$$

We use the mass function introduced by del Popolo (PO mass function)[19]

$$\begin{aligned} \nu f(\nu) &= 1.75 \sqrt{\frac{0.707\nu}{2\pi}} \left[1 + \frac{0.1218}{(0.707\nu)^{0.585}} + \frac{0.0079}{(0.707\nu)^{0.4}} \right] \\ &\times \exp \left[-0.4019 \times 0.707\nu \left(1 + \frac{0.5526}{(0.707\nu)^{0.585}} + \frac{0.02}{(0.707\nu)^{0.4}} \right)^2 \right], \end{aligned} \quad (36)$$

Also, we use the mass function (YNY mass function) presented in [27]

$$\nu f(\nu) = 0.298 \left[1 + (0.893 \sqrt{\frac{\nu}{2}})^{1.39} \right] \nu^{(\frac{0.408}{2})} \exp \left[- (0.893 \sqrt{\frac{\nu}{2}})^2 \right]. \quad (37)$$

Now, we represent the evolution of the ST mass function with respect to k ($k = \log(\frac{M}{M_8})$) in Fig.7 for the tachyon scalar field model and the ΛCDM model. We can see that the evolution of ST mass function with respect to k is the same for tachyon scalar field and the ΛCDM models in the $z = 0$ case, but it is different for tachyon scalar field and ΛCDM models in the $z = 1$ case.

Using Eqs. (30) and (35), for the tachyon scalar field model and the ΛCDM model, we obtain the average comoving number density of halos of mass M in the cases $z = 0, 1$. In Fig.8, we can see explicitly the differences for the cases $z = 0$ and $z = 1$. We can see that difference of the number densities of halo objects is negligible for small objects in the case $z = 1$. Therefore, we can obtain the number density of halo objects for high mass, and we find that the number of objects per unit mass is increasing for high mass in the tachyon scalar field model. Also, using Eqs. (35), (36) and (37), we can compare the various mass functions at $k = 0$ in Fig.9. We can see that the PO mass function is larger than ST mass function and YNY mass function for all mass scales.

VII. CONCLUSION

In this paper, we have studied the evolution of spherical overdensities in tachyon scalar field model by assuming a particular potential and the scale factor with power law behavior. We have shown the evolution of the EoS parameter, the evolution of the density parameter and the evolution of the dimensionless Hubble parameter of tachyon scalar field model with respect to a function of z , for a typical value $n = 1$. We have

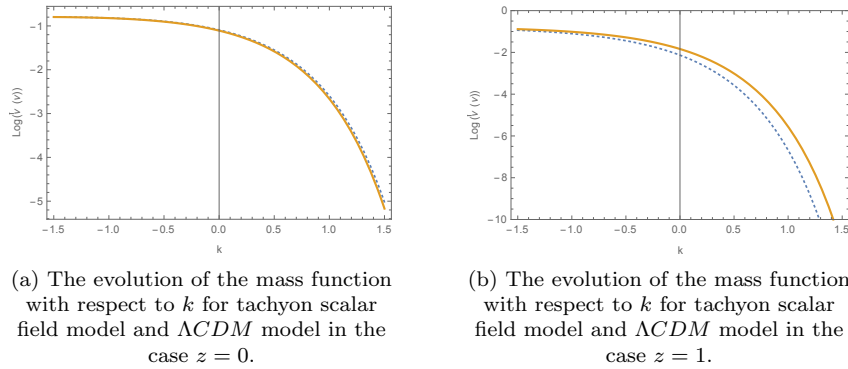


FIG. 7: The thick line represents the tachyon scalar field model for $n = 1$ and The dotted line indicates the Λ CDM model.

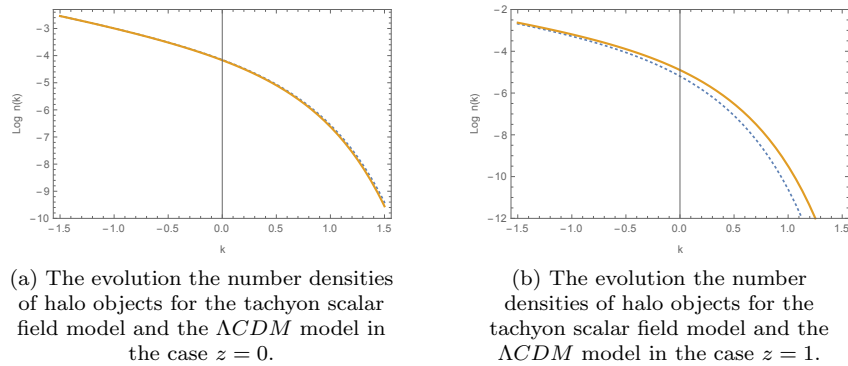


FIG. 8: The thick line represents the tachyon scalar field model for $n = 1$ and the dotted line indicates the Λ CDM model.

also shown that at early times of the scale factor evolution, the growth factor in the tachyon scalar field model drives faster than the EdS and Λ CDM models. So, it is concluded that in the tachyon scalar field model the structure formation may occur sooner than in the other models. At later times, however, we have shown that the growth factor in the tachyon scalar field model drives more slower than that of EdS model. Also, in the EdS model, δ_c is independent of the redshift and thus it has a constant value $\delta_c = 1.686$. In the Λ CDM model, δ_c is smaller than 1.686, but the time evolution of the linear overdensity approaches the

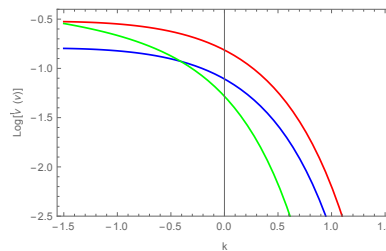


FIG. 9: The evolution of the various mass functions with respect to k for the tachyon scalar field model, $n = 1$, in the case $z = 0$. The blue thick line represent ST mass function, the red thick line represent PO mass function and the green thick line represent YNY mass function

value of EdS model at high redshifts. In fact, at high redshifts, we have a matter dominated universe (dust matter), but at lower redshifts we have a dark energy dominated universe, thus the structure formation occurs earlier. In the tachyon scalar field model, δ_c is driven more slower than that of Λ CDM and EdS models, because in figure (1), the Hubble parameter in the tachyon scalar field model is larger than that of Λ CDM model.

Also, we have shown that in the EdS model, $\lambda(z_c)$ is independent of the redshift, thus it has a constant value i.e. $\lambda = 0.5$. Moreover, the size of structures in the Λ CDM model was larger than that of tachyon scalar field model. In the EdS model, $\xi(z_c)$ is independent of the redshift, hence it has a constant value i.e. $\xi = 5.6$. We have shown that in tachyon scalar field model, the overdense spherical regions with respect to z_c are denser than those of Λ CDM and EdS models. In the EdS model, $\Delta_V(z_c)$ is independent of the redshift, so it has a constant value, $\Delta_V = 178$. The evolution of virial overdensity parameter $\Delta_V(z_c)$ is the main quantity for the halo size. Therefore, we have found that in the tachyon scalar field model the halo size is larger than the EdS and Λ CDM models.

Finally, we have shown that the evolution of the ST mass function with respect to k is the same for tachyon scalar field and Λ CDM models in the $z = 0$ case, but it is not the same for tachyon scalar field model and the Λ CDM model in the $z = 1$ case. Also, the evolution of the number density with respect to k is the same for the tachyon scalar field and Λ CDM models in the $z = 0$ case, but its evolution is not the same for the tachyon scalar field and Λ CDM models in the $z = 1$ case. The difference of number densities of halo objects is negligible for small objects in the $z = 1$ case. Therefore, in obtaining the number density of halo objects for high mass, we find that the number of objects per unit mass is increasing for high mass in the tachyon scalar field model.

Appendix I

The Lagrangian of tachyon scalar field over a cosmological background is given by [28]

$$\mathcal{L} = -V(\phi)\sqrt{1 - \partial_\alpha\phi \partial^\alpha\phi}, \quad (38)$$

where ϕ and $V(\phi)$ are the tachyon scalar field and tachyon potential, respectively. One can obtain the energy-momentum tensor of the tachyon scalar field as follows [31]

$$T_{\mu\nu} = \frac{V(\phi)\partial_\mu\phi\partial_\nu\phi}{\sqrt{1 + g^{\alpha\beta}\partial_\alpha\phi\partial_\beta\phi}} - g_{\mu\nu}V(\phi)\sqrt{1 + g^{\alpha\beta}\partial_\alpha\phi\partial_\beta\phi}. \quad (39)$$

Now, considering (39) as describing a perfect fluid, the energy density ρ and the pressure p for the tachyon scalar field are given by

$$\rho = -T_0^0 = \frac{V(\phi)}{\sqrt{1 - \dot{\phi}^2}},$$

$$p = T_i^i = -V(\phi)\sqrt{1 - \dot{\phi}^2}.$$

The fundamental equations for cosmic fluid in Newtonian gravity are defined as follows [13]

$$\frac{\partial\rho}{\partial t} + \nabla_{\vec{r}} \cdot (\rho\vec{v}) + \frac{p}{c^2} \nabla_{\vec{r}} \cdot \vec{v} = 0, \quad (40)$$

$$\frac{\partial\vec{v}}{\partial t} + (\vec{v} \cdot \nabla_{\vec{r}})\vec{v} + \nabla_{\vec{r}}\Phi + \frac{c^2 \nabla_{\vec{r}} p + \vec{v}\dot{p}}{\rho c^2 + p} = 0, \quad (41)$$

$$\nabla^2 \Phi = 4\pi G \left(\rho + \frac{3p}{c^2} \right), \quad (42)$$

$$\dot{\rho} + 3H\left(\bar{\rho} + \frac{p}{c^2}\right) = 0, \quad (43)$$

where \vec{v} is the velocity in three-space, Φ is the Newtonian gravitational potential, \vec{r} is the physical coordinate and $\bar{\rho}$ is the density of cosmic background. Now, we use the comoving coordinates as follows [13]:

$$\vec{r} = a\vec{x}. \quad (44)$$

Here \vec{r} , a and \vec{x} are the physical coordinates, the scale factor and the comoving coordinates, respectively. Taking time derivative of Eq. (44), one can obtain

$$\vec{v}(\vec{x}, t) = a \left[H(a)\vec{x} + \vec{u}(\vec{x}, t) \right], \quad (45)$$

where

$$\vec{v}(\vec{x}, t) = \frac{dr(\vec{x}, t)}{dt}, \quad (46)$$

$$\vec{u}(\vec{x}, t) = \frac{dx(\vec{x}, t)}{dt}. \quad (47)$$

Here, $H(a)$ is the Hubble function and $\vec{u}(\vec{x}, t)$ is the comoving peculiar velocity. Next, one can introduce the following definitions

$$\nabla_{\vec{r}} = \frac{1}{a} \nabla_{\vec{x}}, \quad (48)$$

$$\left. \frac{\partial}{\partial t} \right|_r = \left. \frac{\partial}{\partial t} \right|_x - \frac{1}{a} \vec{v} \cdot \nabla_{\vec{x}}, \quad (49)$$

$$\rho(\vec{x}, t) = \bar{\rho}(1 + \delta(\vec{x}, t)), \quad (50)$$

$$p = \omega\rho(\vec{x}, t)c^2, \quad (51)$$

$$\Phi(\vec{x}, t) = \Phi_0(\vec{x}, t) + \phi(\vec{x}, t), \quad (52)$$

where ω is the equation of state parameter. Now, using Eqs. (45), (48), (49), (50), (51), (52) and inserting Eqs. (40), (41), (42) and (43), one can obtain [13]

$$\dot{\delta} + (1 + \omega)(1 + \delta) \nabla_{\vec{x}} \cdot \vec{u} = 0, \quad (53)$$

$$\frac{\partial \vec{u}}{\partial t} + 2H\vec{u} + (\vec{u} \cdot \nabla_{\vec{x}})\vec{u} + \frac{1}{a^2} \nabla_{\vec{x}} \phi = 0, \quad (54)$$

$$\nabla_{\vec{x}}^2 \phi - 4\pi G(1 + 3\omega)a^2\bar{\rho}\delta = 0. \quad (55)$$

We take the divergence of the Eq. (54) and represent the analysis [13]

$$\nabla \cdot [(\vec{u} \cdot \nabla)\vec{u}] = \frac{1}{3}\theta^2 + \sigma^2 - w^2, \quad (56)$$

where

$$\theta = \nabla_{\vec{x}} \cdot \vec{u}, \quad (57)$$

$$\sigma_{ij} = \frac{1}{2} \left(\frac{\partial u^j}{\partial x^i} + \frac{\partial u^i}{\partial x^j} \right) - \frac{1}{3} \theta \delta_{ij}, \quad (58)$$

$$w_{ij} = \frac{1}{2} \left(\frac{\partial u^j}{\partial x^i} - \frac{\partial u^i}{\partial x^j} \right), \quad (59)$$

Here, $\sigma^2 = \sigma_{ij}\sigma^{ij}$ is the shear tensor and $w^2 = w_{ij}w^{ij}$ is the rotation tensor. Taking time derivative of Eq. (53) and using Eqs. (53), (54), (55) and (56), one can obtain [13]

$$\ddot{\delta} + \left(2H - \frac{\dot{\omega}}{1+\omega} \right) \dot{\delta} - \frac{4+3\omega}{3(1+\omega)} \frac{\dot{\delta}^2}{1+\delta} - 4\pi G\bar{\rho}(1+\omega)(1+3\omega)\delta(1+\delta) - (1+\omega)(1+\delta)(\sigma^2 - w^2) = 0. \quad (60)$$

Now, we can introduce the following definition

$$\frac{\partial}{\partial t} = aH(a) \frac{\partial}{\partial a}. \quad (61)$$

Using Eq. (61) and inserting Eq. (60), one can rewrite Eq. (60) as follows [13]

$$\delta'' + \left(\frac{3}{a} + \frac{E'}{E} - \frac{\omega'}{1+\omega} \right) \delta' - \frac{4+3\omega}{3(1+\omega)} \frac{\delta'^2}{1+\delta} - \frac{3}{2} \frac{\Omega_{fluid,0}}{a^2 E^2(a)} h(a)(1+\omega)(1+3\omega)\delta(1+\delta) - \frac{1}{aH^2(a)} (1+\omega)(1+\delta)(\sigma^2 - w^2) = 0, \quad (62)$$

where $E = H/H_0$ is the dimensionless Hubble parameter, $\Omega_{fluid,0} = 8\pi G\bar{\rho}/3H^2$ is the density parameter of the fluid at $a_0 = 1$, $h(a)$ is a function that describes the time evolution of dark energy with scale factor, H_0 is the Hubble parameter at the present time and the prime sign denotes the derivative with respect to the scale factor.

For the collapse of a homogeneous sphere, one can ignore the shear and rotation tensors. Also, we limit ourselves to the spherical perturbation filled with dust $\omega = 0$, for which

$$h(a) = a^{-3}.$$

Therefore, one can obtain the non-linear and linear perturbation equations as follows [13], [32]

$$\delta'' + \left(\frac{3}{a} + \frac{E'}{E} \right) \delta' - \frac{4}{3} \frac{\delta'^2}{1+\delta} - \frac{3}{2} \frac{\Omega_{m_0}}{a^5 E^2(a)} \delta(1+\delta) = 0, \quad (63)$$

$$\delta'' + \left(\frac{3}{a} + \frac{E'}{E} \right) \delta' - \frac{3}{2} \frac{\Omega_{m_0}}{a^5 E^2(a)} \delta = 0. \quad (64)$$

Appendix II

In the numerical study of solving Eqs. (21) and (22), we have used the procedure used in Ref.[13] to obtain the initial conditions for drawing the curves of figure 3, in tachyon scalar field model, as follows

$$g(a_i) = 3.615 \times 10^{-4}, \quad g'(a_i) = 0, \quad a_i = 10^{-4}. \quad (65)$$

The scale factor a at the redshift z is defined as follows

$$a = (1+z)^{-1}. \quad (66)$$

Taking derivative of Eq. (66), one can obtain

$$\frac{d}{dz} = -a^2 \frac{d}{da}. \quad (67)$$

Using Eqs. (8), (19) and (67) and inserting Eqs. (14), (15), we can obtain

$$\frac{d\Omega_\Lambda}{da} + \frac{3\Omega_\Lambda}{a} (1 - \Omega_\Lambda) \left(\frac{2}{3n} - 1 \right) = 0, \quad (68)$$

$$\frac{dE}{da} + \frac{3}{2} \frac{E}{a} \left[1 + \Omega_\Lambda \left(\frac{2}{3n} - 1 \right) \right] = 0. \quad (69)$$

Using Eqs. (68), (69), (65) and inserting Eq. (22), we can plot the curve of figure (3 – a) for tachyon scalar field model using the “Mathematica” in the linear case. Also, using Eqs. (5), (9), (10) and $\rho_m = \rho_{m_0} a^{-3}$ and $\rho_\Lambda = \rho_{\Lambda_0} a^{-3(1+\omega_\Lambda)}$, one can obtain

$$E(a) = \sqrt{\Omega_{m_0} a^{-3} + \Omega_{\Lambda_0} a^{-3(1+\omega_\Lambda)}}. \quad (70)$$

Also, using Eqs. (19), (65), (70) and inserting Eq. (21), we can plot the curve of figure (3 – b) for tachyon scalar field model using the “Mathematica” in the non-linear case.

Acknowledgment

We would like to thank M. Malekjani for giving us useful comments that helped us to improve the scientific content of the manuscript.

-
- [1] Abramo. L. R., Batista. R. C., Liberato. L., Rosenfeld. R., 2007, JCAPP, 11, 12.
 - [2] Avelino. P. P, Losano. L, Rodrigues. J. J, 2011, Phys. Lett. B 699, 10.
 - [3] Bond. R. J., Cole. S., Efstathiou. G., Kaiser. N. 1991, ApJ, 379 ,440.
 - [4] Bernardeau. F. 1994, ApJ, 433, 1.
 - [5] Bernardis. P. De., et al. 2000, Nature 404, 955;
Perlmutter. S., et al. 2003, Astrophys. J. 598, 102;
Seljak. U., et al. 2005, Phys. Rev. D 71, 103515.
 - [6] Cai. Y. F., Saridakis. E. N., Setare. M. R., Xia. J. Q., 2010, Phys. Rept. 493, 1.
 - [7] Copeland. E. J., Sami. M., Tsujikawa. T. S. 2006, IJMPD, 15, 1753.
 - [8] Doran. M., Robbers. G. 2006, JCAPP, 6, 26;
Wetterich. C. 2004, Phys. Lett. B, 594, 17.
 - [9] Fillmore. A. J., Goldreich. P. 1984, ApJ, 281, 1.
 - [10] Gunn. J. E., Gott. R. J. 1972, ApJ, 176,1.
 - [11] Hoffman. Y., Shaham. J. 1985, ApJ. 297, 16.
 - [12] Meyer. S., Pace. F., Bartelmann. M. 2012, Phys.Rev.D, 86, 103002.
 - [13] Pace. F., Waizmann. J. C., Bartelmann. M., 2010, MNRAS, 406, 1865.
 - [14] Pace. F., Moscardini. L, Crittenden. R., Bartelmann. M., Pettorino. V. 2014, MNRAS, 437, 547.
 - [15] Padmanabhan. T. 1996, Cosmology and Astrophysics through Problems, Cambridge University Press.
 - [16] Padmanabhan. T. 2003, Phys. Rept. 380, 235.
 - [17] Press. H. W., Schechter. P. 1974, ApJ, 187, 425.
 - [18] Percival. W. J. 2005, A. A, 443, 819.
 - [19] Del Popolo. A, 2006, ApJ, 637, 12;
Del Popolo. A, 2006, A. A, 448, 439.
 - [20] Riess. A. G., et al. 1998, Astron. J. 116, 1009;
Perlmutter. S., et al. 1999, Astrophys. J. 517, 565.
 - [21] Ryden. S. B., Gunn. E. J. 1987, ApJ. 318, 15.

- [22] Setare. M. R. 2007, Phys. Lett. B 653,116;
Setare. M. R., Sadeghi. J., Amani. A. R., 2009, Phys. Lett. B 673, 241.
- [23] Sheth. R. K., Tormen. G., 1999, MNRAS, 308, 119;
Sheth. R. K., Tormen. G. 2002, MNRAS, 329, 61.
- [24] Viana. P. T. P., Liddle. A. R., 1996, MNRAS, 281, 323.
- [25] Wang. L., Steinhardt. P. J. 1998, Astro. Phys. J. 508, 483.
- [26] Weinberg. S. 1989, Reviews of Modern Physics, 61, 1.
- [27] Yahagi. H., Nagashima. M., Yoshii. Y. 2004, ApJ, 605, 709.
- [28] Padmanabhan. T, 2002, Phys. Rev. D 66, 021301.
- [29] Malekjani. M, Naderi. T, Pace. F, 2015, MNRAS 453, 4148.
- [30] Naderi. T, Malekjani. M, Pace. F, 2015, MNRAS, 447, 1873.
- [31] Zhang. J, Zhang. X, Liu. H, 2007, Phys. Lett. B 651, 84.
- [32] Malekjani. M., Lu. J, Nazari-Pooya. N., Xu. L, Mohammad-Zadeh Jassur. D., Honari-Jafarpour. M., 2015, Astrophys Space Sci, 360, 24.